

## LHC and Tevatron results on the $t\bar{t}$ differential cross sections

---

**Riccardo Di Sipio\***

*University of Toronto*

*E-mail:* [disipio@cern.ch](mailto:disipio@cern.ch)

This note describes a review of the most recent  $t\bar{t}$  differential cross sections measurement performed by LHC and Tevatron experiments. I will describe the measurements of fiducial and full phase-space differential cross sections based on events with exactly two, one or zero charged leptons in the final state. These results are compared to predictions made with next-to-leading order or next-to-next-to leading order numerical calculations.

*9th International Workshop on the CKM Unitarity Triangle  
28 November - 3 December 2016  
Tata Institute for Fundamental Research (TIFR), Mumbai, India*

---

\*Speaker.

## 1. Introduction

The top quark, first discovered [1, 2] by the CDF [3] and D0 [4] experiments in 1995, has been observed at CERN by the ATLAS [5] and CMS experiments [6] and now is being studied with large data samples. Several million top-quark pairs have been collected thanks to a trigger and data acquisition overall performance above 90% for both ATLAS and CMS. After data quality requirements, about  $20 \text{ fb}^{-1}$  in 2012 and  $3 \text{ fb}^{-1}$  in 2015 were made available for the physics analyses for each experiment.

It is of great interest to study the differential cross-sections of top-quark pairs to constrain Monte Carlo models [7, 8, 10, 11], parton distribution functions [9] and other theoretical assumptions. The measurements performed by ATLAS and CMS at  $\sqrt{s} = 7 \text{ TeV}$ ,  $\sqrt{s} = 8 \text{ TeV}$  and  $\sqrt{s} = 13 \text{ TeV}$  are in good agreement with several Monte Carlo models for the  $t\bar{t}$  invariant mass, transverse momentum and rapidity distributions. Discrepancies have been observed in particular in the top-quark transverse momentum distribution. To further constrain the perturbative QCD models, the  $t\bar{t}$ +jets production has been studied by ATLAS and CMS.

## 2. Kinematic reconstruction

Ideally, the kinematics of the top-quarks pair produced in the hard-scattering process is ultimately what experimentalist would like to measure to compare with the theoretical predictions. In order to do so, unfolded cross-section distributions are compared to next-to-next-to-leading order calculations, which to this date are not yet matched to parton shower algorithms. Differential cross-sections are often strongly dependent on the details of the calculation. Moreover, Monte Carlo generators have to be used to evaluate the efficiency, acceptance and matching corrections where applicable. Usually, this procedure results in large systematic uncertainties.

On the other hand, what is actually observed experimentally are the kinematics of the final-state objects such as leptons, jets and neutrinos, which arise from the decay of the top-quark pair, as well as additional jets arising from QCD radiation. The so-called "fiducial phase-space" measurements are based on final-state objects only, in order to minimize the extrapolations between measurement and predictions. Usually, these measurements present smaller systematic uncertainties. Depending on the decay channel, different reconstruction techniques are deployed:

**Single lepton (resolved kinematics)** The decay chain is reconstructed by identifying all of the final-state objects separately and applying kinematic constraints such as the invariant mass of the  $W$  boson and of the top quark. The so-called "PseudoTop" algorithm has been agreed upon between theorists and experimentalists, and has been implemented, for example, in Rivet [13] routines. Measurements performed in this channel [14, 17, 16, 18, 19, 21] fully reconstruct the top-quarks' four momenta with good resolution at low- $p_T$ , but are limited by uncertainties in jet energy scale and resolution, flavour-tagging efficiency and signal modelling.

**Single lepton (boosted kinematics)** The decay chain of the top quark decaying leptonically is reconstructed by applying kinematic constraints. The invariant mass of the  $W$  boson is used to find the most probable value of the longitudinal component of the neutrino four-momentum.

If the top quark decaying hadronically has a transverse momentum  $p_T \geq 250$  GeV, it can be reconstructed using a large-radius jet. Subsequently, substructure variables are used to determine whether the jet is a top-quark candidate. Measurements performed in this channel [14, 15, 20] have the ability to explore the very high- $p_T$  region, but are limited by statistics and uncertainties in jet energy scale, flavour-tagging efficiency and signal modelling.

**Di-lepton (resolved kinematics)** The four-momenta of the two top quarks are reconstructed by applying kinematic constraints to stable final-state particles to find the optimal longitudinal component of the momenta of the two neutrinos in the final state ("neutrino weighting") [12]. Measurements performed in this channel [22, 25, 26, 19, 23, 24, 28] have a very low background but have worse resolution due to the presence of two neutrinos. These measurements are limited by statistics and uncertainties in flavour-tagging efficiency and signal modelling.

**All-hadronic (boosted kinematics)** In this case the kinematic reconstruction is straightforward, as the hadronic decay of a both high- $p_T$  top quarks are contained in large-radius jets. Top-tagging algorithms based on jet substructure variables are deployed to separate the  $t\bar{t}$  signal from the multi-jet background. Measurements performed in this channel [29, 30, 31] have the ability to explore a  $p_T$  region much higher than the other channels, but are limited by statistics and uncertainties in jet energy and mass scale and resolution, flavour-tagging efficiency and signal modelling.

After the kinematic reconstruction, an unfolding procedure is applied to correct for distortions due to the detector response and event selection. Fiducial and full phase-space unfolded differential cross-sections are usually stored in the HEPData database<sup>1</sup>. This allows theorists to compare experimental data against predictions made with Monte Carlo generators, and ensure the accessibility of measurements.

### 3. Full and Fiducial phase-space cross-sections

The top-quark transverse momentum distribution is probably the most important observable. In fact, it is sensitive to final state radiation, which tests the QCD calculations that model this effect. Moreover, in order to perform this measurement up to about 1 TeV, different reconstruction methods have to be deployed to cope with the different kinematic regimes. Not surprisingly, many sources indicate a disagreement between data and LO and NLO predictions, which is especially evident for  $p_T \geq 300$  GeV [22, 26]. However, the comparison of full phase-space differential cross-sections to NNLO calculations (Figure 1) shows better agreement, indicating that higher-order corrections have a large impact.

The invariant mass of the  $t\bar{t}$  system is often regarded as one of the more intriguing observables. In fact, any appearance of "bumps" or "dips" in its spectrum can signal the presence of resonant states or interference not accounted for in the Standard Model. The agreement between data and NNLO calculations seems satisfactory [16, 18] despite the increasing statistical and systematic

<sup>1</sup><https://hepdata.net>

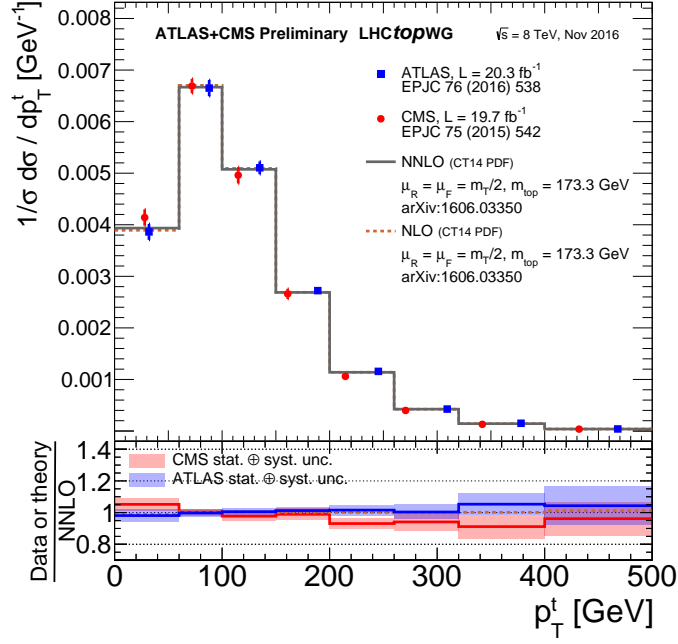


**Figure 1:** Full phase-space normalised differential  $t\bar{t}$  cross-section as a function of the transverse momentum of the top quark in the single-lepton channel. The CMS and ATLAS results are compared to the NLO and NNLO calculations. The values for the top-quark mass ( $m_{\text{top}}$ ), the renormalisation ( $\mu_R$ ) and factorisation ( $\mu_F$ ) scales, and the choice of the PDF set used in each calculation are provided. The variable  $m_T$  is defined as the square root of the sum of the squares of top-quark mass and the transverse momentum of the top quark. The shaded bands show the total uncertainty on the data measurements in each bin. The lower panel shows the ratio of the data measurements and the NLO calculation to the NNLO calculation.

uncertainties at invariant masses larger than about 1 TeV (Figure 2). However, the current resolution limits bump hunting. In this case, the all-hadronic boosted channel may be promising thanks to the kinematic resolution [29, 30].

The transverse momentum of the  $t\bar{t}$  system is sensitive to additional radiation (e.g. initial-state radiation). The comparison against Monte Carlo generators with NLO accuracy shows that the recoil of the  $t\bar{t}$  system is overestimated for  $p_T^{t\bar{t}} \geq 100$  GeV (Figure 3).

The rapidity of the  $t\bar{t}$  system is sensitive to different choices of parton distribution functions. This appears clearly in double-differential cross-sections, where the rapidity of the  $t\bar{t}$  system is measured as a function of the invariant mass [27]. A tendency to overestimate the production at high  $|\eta|$  is observed [16, 19], but it can be also interpreted in terms of an inadequate extrapolation of the parton distribution functions in the more forward region.

Finally, additional radiation (I/FSR) produced along with the top-quark pair is a critical test of NLO corrections, parton shower models and matrix-element-to-parton-shower matching schemes. The extra jet activity [24, 28] is used to constrain  $t\bar{t}$  production models as implemented in Monte Carlo generators.

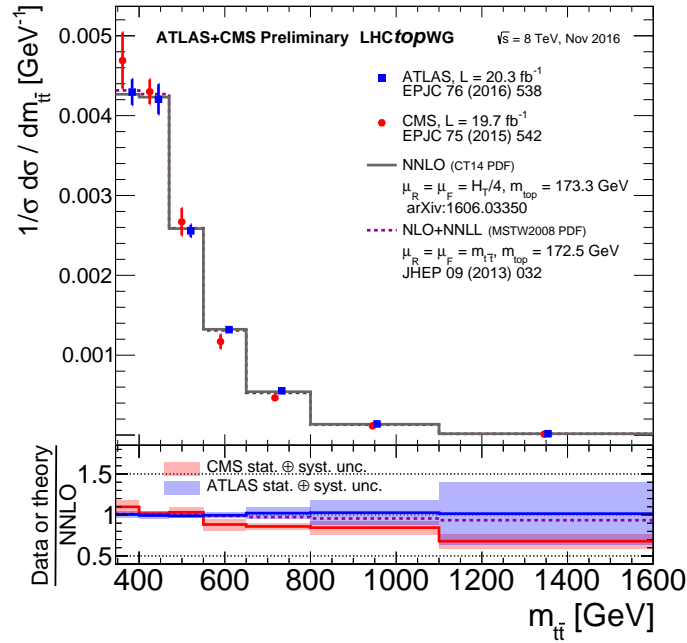


**Figure 2:** Full phase-space normalised differential  $t\bar{t}$  cross-section as a function of the invariant mass of the top-quark pair in the single-lepton channel. The CMS and ATLAS results are compared to NNLO and NLO+NNLL calculations. The values for the top-quark mass ( $m_{\text{top}}$ ), the renormalisation ( $\mu_R$ ) and factorisation ( $\mu_F$ ) scales, and the choice of the PDF set used in each calculation are provided. The shaded bands show the total uncertainty on the data measurements in each bin. The lower panel shows the ratio of the data measurements and the NLO+NNLL calculation to the NNLO calculation.

#### 4. Conclusions

Top-quark pair differential cross-sections are instrumental to constrain NLO generators (particle level) and NNLO calculations (parton level), and search for beyond-Standard-Model physics. In particular, it is observed that NNLO corrections improve data/theory agreement in differential cross-section as a function of the top-quark transverse momentum. The field is now entering the era of boosted top-quarks and double-differential cross-sections measurements.

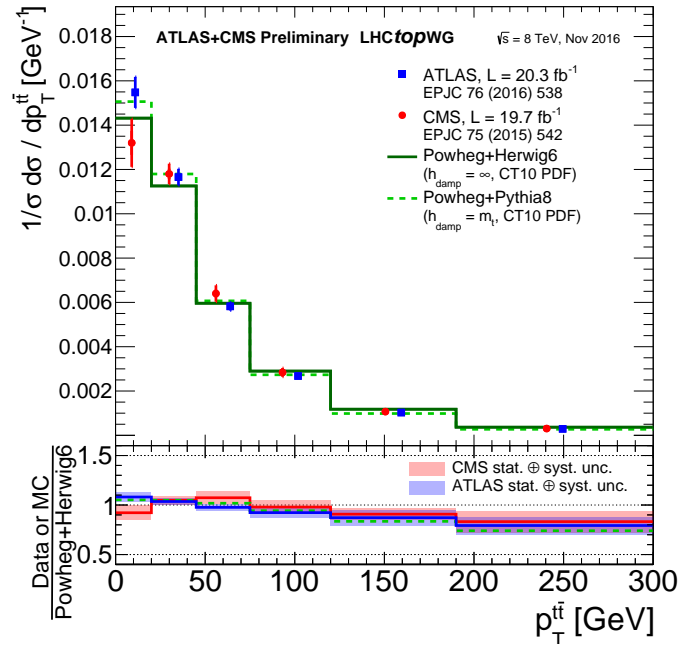


**Figure 3:** Full phase-space normalised differential  $t\bar{t}$  cross-section as a function of the transverse momentum of the top-quark pair. The CMS and ATLAS results are compared to predictions from the Powheg+Herwig6 and Powheg+Pythia8 MC generators. The shaded bands show the total uncertainty on the data measurements in each bin. The lower panel shows the ratio of the data measurements and the Powheg+Pythia8 prediction to the Powheg+Herwig6 prediction.

## References

- [1] Observation of Top Quark Production in  $p\bar{p}$  Collisions with the Collider Detector at Fermilab, The CDF Collaboration, Phys. Rev. Lett. 74 (1995) 2626 .
- [2] Observation of the Top Quark, The D0 Collaboration, Phys. Rev. Letters (74) 2632 .
- [3] The CDF Detector: an overview, The CDF Collaboration, Nucl. Instr. and Methods, A271 (387-403) (1988) .
- [4] The D0 Detector, The D0 Collaboration, Nucl. Instr. and Methods, A338, 185 (1994) .
- [5] The ATLAS Experiment at the CERN Large Hadron Collider, The ATLAS Collaboration, JINST 3 (2008) S08003 .
- [6] The CMS experiment at the CERN Large Hadron Collider, The CMS Collaboration, 2008 JINST 3 S08004 .
- [7] S. Frixione, P. Nason and G. Ridolfi, A positive-weight next-to-leading-order Monte Carlo for heavy flavour hadroproduction, JHEP 09 (2007) 126 .
- [8] S. Frixione, P. Nason and B. R. Webber, Matching NLO QCD and parton showers in heavy flavor production, JHEP 08 (2003) 007 .
- [9] J. Butterworth et al., PDF4LHC recommendations for LHC Run II, J. Phys. G: Nucl. Part. Phys. 43 023001 (2016) .
- [10] T. Sjöstrand, S. Mrenna and P.Z. Skands, A Brief Introduction to PYTHIA 8.1, Comput. Phys. Commun. 178 p. 852-867 (2008) .
- [11] Bähr et al., Herwig++ physics and manual, Eur.Phys.J. C58 (2008) no. 4, 639–707 .
- [12] Precise measurement of the top quark mass in dilepton decays using optimized neutrino weighting, The D0 Collaboration, PLB 752, 18 (2016) .
- [13] Rivet user manual, A. Buckley et al., arXiv:1003.0694 .
- [14] Measurements of top-quark pair differential cross-sections in the lepton+jets channel in  $pp$  collisions at  $\sqrt{s} = 13$  TeV using the ATLAS detector, The ATLAS Collaboration, ATLAS-CONF-2016-040.
- [15] Measurement of the differential cross-section of highly boosted top quarks as a function of their transverse momentum in  $\sqrt{s} = 8$  TeV in proton-proton collisions using the ATLAS detector, The ATLAS Collaboration, Phys. Rev. D 93, 032009.
- [16] Measurements of top-quark pair differential cross-sections in the lepton+jets channel in  $pp$  collisions at  $\sqrt{s} = 8$  TeV using the ATLAS detector, The ATLAS Collaboration, Eur.Phys.J. C76 (2016) no.10, 538.
- [17] Measurement of the inclusive and differential  $t\bar{t}$  production cross sections in lepton + jets final states at  $\sqrt{s} = 13$  TeV, The CMS Collaboration, CMS-PAS-TOP-16-008.
- [18] Measurement of the differential cross sections for top quark pair production as a function of kinematic event variables in  $pp$  collisions at  $\sqrt{s} = 7$  and 8 TeV, The CMS Collaboration, Phys. Rev. D 94, 052006 .
- [19] Measurement of the differential cross section for top quark pair production in  $pp$  collisions at  $\sqrt{s} = 8$  TeV, The CMS Collaboration, EPJC 75(2015)542 .
- [20] Measurement of the integrated and differential  $t\bar{t}$  production cross sections for high- $p_T$  top quarks in  $pp$  collisions at  $\sqrt{s} = 8$  TeV, The CMS Collaboration, Phys. Rev. D 94, 072002 .

- [21] Dependence of the  $t\bar{t}$  production cross section on the transverse momentum of the top quark, The D0 Collaboration, Phys.Lett.B693:515-521, 2010 .
- [22] Measurements of top-quark pair differential cross-sections in the  $e\mu$  channel in  $pp$  collisions at  $\sqrt{s} = 13$  TeV using the ATLAS detector, The ATLAS Collaboration, arXiv:1612.05220 .
- [23] Measurement of top quark pair differential cross sections in the dilepton channel in  $pp$  collisions at  $\sqrt{s} = 7$  and 8 TeV ATLAS, The ATLAS Collaboration, Phys. Rev. D 94, 092003 .
- [24] Measurement of jet activity produced in top-quark events with an electron, a muon and two  $b$ -tagged jets in the final state in  $pp$  collisions at  $\sqrt{s} = \text{TeV}$  with the ATLAS detector, The ATLAS Collaboration, arXiv:1610.09978 .
- [25] Measurement of particle level differential  $t\bar{t}$  cross sections in the dilepton channel at  $\sqrt{s} = 13$  TeV, The CMS Collaboration, CMS-PAS-TOP-16-007 .
- [26] Measurement of the differential cross section for  $t\bar{t}$  production in the dilepton final state at  $\sqrt{s} = 13$  TeV, The CMS Collaboration, CMS-PAS-TOP-16-011 .
- [27] Measurement of double differential cross sections for top quark pair production in  $pp$  collisions at  $\sqrt{s} = 8$  TeV, The CMS Collaboration, CMS-PAS-TOP-14-013 .
- [28] Measurement of  $t\bar{t}$  production with additional jet activity, including  $b$ -quark jets, in the dilepton decay channel using  $pp$  collisions at  $\sqrt{s} = 8$  TeV, The CMS Collaboration, EPJC 76(2016)379 .
- [29] Measurements of  $t\bar{t}$  differential cross-sections in the all-hadronic channel with the ATLAS detector using highly boosted top quarks in  $pp$  collisions at  $\sqrt{s} = 13$  TeV, The ATLAS Collaboration, ATLAS-CONF-2016-100 .
- [30] Measurement of the  $t\bar{t}$  production cross section at  $\sqrt{s} = 13$  TeV in the all-jets final state, The CMS Collaboration, CMS-PAS-TOP-16-013 .
- [31] Measurement of the  $t\bar{t}$  production cross section in the all-jets final state in  $pp$  collisions at  $\sqrt{s} = 8$  TeV, The CMS Collaboration, Eur. Phys. J. C 76 (2016) 128 .